Human Molecular Genetics, 2011, Vol. 20, No. 5 **1016–1025**
doi:10.1093/hmg/ddq547
Advance Access published on December 20, 2010

MSX1 and *TGF-β3* are novel target genes functionally regulated by FOXE1

Isabella Venza[1,†], Maria Visalli[2,†], Luca Parrillo[4], Mario De Felice[4], Diana Teti[2,*] and Mario Venza[3]

[1]Department of Surgical Specialities, [2]Department of Experimental Pathology and Microbiology and [3]Department of Odontostomatology, University of Messina, Italy and [4]IRGS-Biogem, Ariano Irpino (Av), Italy

Received November 20, 2010; Revised and Accepted December 13, 2010

***FOXE1* mutations cause the Bamforth–Lazarus syndrome characterized by thyroid and craniofacial defects. Although a pioneer activity of FOXE1 in thyroid development has been reported, FOXE1 regulation in other contexts remains unexplored. We pointed to: (i) a role of FOXE1 in controlling the expression of *MSX1* and *TGF-β3* relevant in craniofacial development and (ii) a causative part of *FOXE1* mutations or mice *Foxe1*$^{-/-}$ genotype in the pathogenesis of cleft palate in the Bamforth–Lazarus syndrome. The *MSX1* and *TGF-β3* up-regulation in response to FOXE1 at both transcriptional and translational levels and the recruitment of FOXE1 to specific binding motifs, together with the transactivation of the promoters of these genes, indicate that *MSX1* and *TGF-β3* are direct FOXE1 targets. Moreover, we showed that all the known forkhead-domain mutations, but not the polyalanine-stretch polymorphisms, affect the FOXE1 ability to bind to and transactivate *MSX1* and *TGF-β3* promoters. In 14-day *Foxe1*$^{-/-}$ mice embryos, Tgf-β3 and Msx1 mRNAs were almost absent in palatal shelves compared with *Foxe1*$^{+/-}$ embryos. Our findings give new insights into the genetic mechanisms underlying the Bamforth–Lazarus syndrome-associated facial defects.**

INTRODUCTION

The mammalian Forkhead Box (FOX) family of transcription factors consists of more than 50 proteins characterized by an evolutionarily conserved winged helix DNA-binding domain. Some forkhead genes are key regulators of embryogenesis and play important roles in cell differentiation and development, hormone responsiveness and aging (1–4). The sensitivity of human developmental processes, including immune, skeletal, circulatory, eye and skin defects, to alterations in forkhead gene dosage is well documented (5).

The gene *Foxe1*, formerly named *thyroid transcription factor 2* (*ttf2*), contains a single coding exon (6) and is located in mice on chromosome 4 (7). The human ortholog *FOXE1* is mapped to the q22 region of chromosome 9 (6). During mouse embryogenesis, Foxe1 is expressed in the foregut endoderm, in the craniopharyngeal ectoderm involved in palate formation and in the thyroid primordium (7,8). Human FOXE1 expression was detected in the oropharyngeal epithelium and thymus later than in the mouse (9). Homozygous null mice with targeted disruption of *Foxe1* exhibit severe cleft palate and sublingual or completely absent thyroid gland (10). Homozygous, human loss-of-function mutations located within the forkhead domain of *FOXE1* cause the Bamforth–Lazarus syndrome (OMIM 241850), which includes congenital hypothyroidism, cleft palate and spiky hair, with or without choanal atresia, bifid epiglottis and ocular hypertelorism, depending on the severity of the mutation (11–15). Functional studies *in vitro* indicated that the F137S (12), R102C (13) and A65V (15) FOXE1 mutant proteins exhibit complete loss of DNA-binding and transcriptional ability, whereas the S57N mutant (14) retains some specific DNA-binding and transcriptional activating function. Studies in thyroid cells indicate that Foxe1 is required for the expression of thyroid-specific genes, such as *thyroglobulin* (*Tg*) and *thyroid peroxidase* (*TPO*) (16–21), thus explaining the variable pathologies associated with thyroid development and function. On the other hand, the constant presence of cleft palate and the frequent choanal atresia, bifid epiglottis and ocular abnormalities observed in the Bamforth–Lazarus syndrome strongly suggest that *FOXE1* controls downstream genes required for craniofacial morphogenesis.

*To whom correspondence should be addressed at: Dipartimento di Patologia e Microbiologia Sperimentale, Sezione di Patologia Sperimentale, Azienda Policlinico Universitario, Torre Biologica—4° piano, via Consolare Valeria, 1, 98125 Messina, Italy. Tel: +39 902213340; Fax: +39 902213341; Email: dteti@unime.it
†The authors wish it to be known that, in their opinion, the first two authors should be regarded as joint First Authors.

Among the critical factors involved in craniofacial development, we have chosen *MSX1* and *TGF-β3* genes since: (i) they are essential for proper palate formation in humans and mice (22–28); (ii) their mutations or changes in expression underlie craniofacial anomalies (29–41); (iii) they harbor a putative *FOXE1* consensus site in their promoter regions. Here, we demonstrated that *MSX1* and *TGF-β3* are novel FOXE1 targets and candidates to cause facial defects in the Bamforth–Lazarus syndrome. We showed the effects of different *FOXE1* forkhead-domain mutations and polyalanine-stretch lengths on the binding ability of this transcription factor to specific regulatory elements within the promoters of *MSX1* and *TGF-β3* and the levels of transcriptional activation. These data have been confirmed by hybridization experiments performed in *Foxe1* null mice.

RESULTS

FOXE1 affects MSX1 and TGF-β3 mRNA levels

To investigate *MSX1* and *TGF-β3* regulation by FOXE1, real-time PCR was performed on cDNA samples from 293 EBNA cells overexpressing wt or mutant FOXE1. Figure 1 shows that untransfected cells expressed basal levels of MSX1 (top panel) and TGF-β3 (bottom panel) transcripts which significantly increased in cells overexpressing wt or variable-polyalanine-stretch-length FOXE1. With respect to wt FOXE1-transfected cells, significantly lower mRNA amounts of MSX1 and TGF-β3 were found in cells overexpressing S57N or R72S mutant FOXE1, whereas insignificant levels of MSX1 and TGF-β3 transcripts were detected in cells overexpressing F137S, R102C and A65V mutant FOXE1. These results suggest that forkhead domain mutations variably affect the ability of FOXE1 to activate *MSX1* and *TGF-β3* expression.

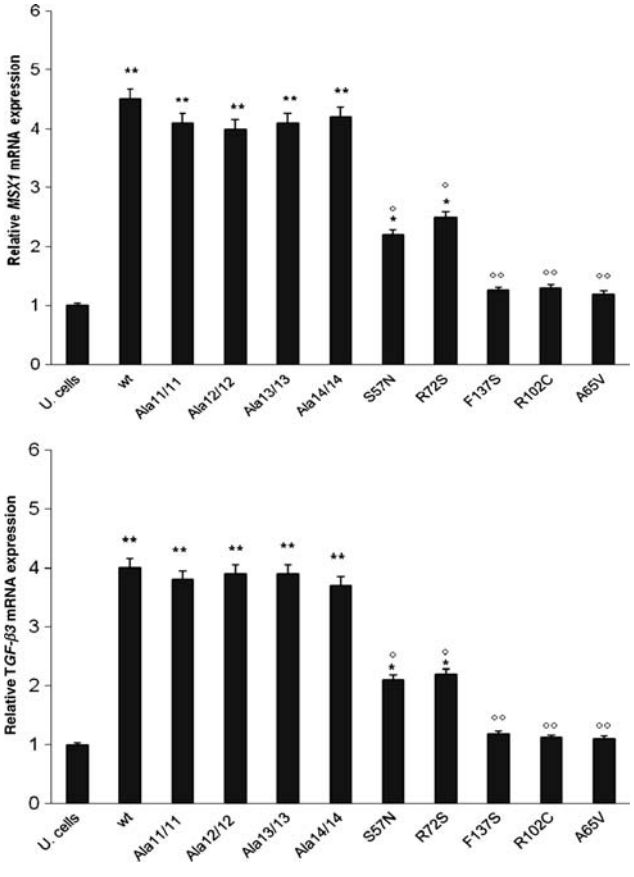

Figure 1. MSX1 and TGF-β3 mRNA levels in 293 EBNA cells co-transfected with wt or mutant FOXE1 expression vectors. Quantification of MSX1 and TGF-β3 mRNAs was performed through real-time PCR. Data represent the average of three independent PCR runs carried out in duplicate. Error bars are given as standard deviation. All results were normalized for total RNA amount using β-actin gene as reference. $^{*}P < 0.05$ and $^{**}P < 0.01$ versus untransfected cells (U. cells), $^{\circ}P < 0.01$ and $^{\circ\circ}P < 0.001$ versus cells transfected with wt FOXE1, based on Student's two-tailed *t*-test.

MSX1 and TGF-β3 protein expression in wt or mutant FOXE1-transfected cells

The 293 EBNA cells were transfected with wt or mutant FOXE1 expression plasmids and assessed for the expression of MSX1 and TGF-β3 proteins by western blotting—the results of which are shown in Figure 2 compared with a housekeeping gene β-actin. Following immunoblotting, in wt and polyalanine-stretch mutant FOXE1-transfected cells, two proteins were identified, migrating with molecular masses of 32 and 50 kDa and corresponding to MSX1 (section A, lanes 2–6) and TGF-β3 (section B, lanes 2–6), respectively. In cells overexpressing S57N and R72S FOXE1, a weaker signal was observed for both the proteins (sections A and B, lanes 7 and 8), whereas no expression of either MSX1 or TGF-β3 was detected in cells transfected with F137S, R102C and A65V FOXE1 mutant plasmids (sections A and B, lanes 9–11). Therefore, the degree of MSX1 and TGF-β3 protein expression induced by wt or mutant FOXE1 follows that observed at the transcriptional level.

Effects of FOXE1 on *MSX1* and *TGF-β3* promoter activity

Transcriptional regulatory function of FOXE1 was tested by co-transfecting into 293 EBNA cells wt or mutant FOXE1 expression plasmids, with luciferase reporter plasmids transcriptionally directed by *MSX1* or *TGF-β3* promoters. Figure 3 shows that transfection of increasing amounts of wt FOXE1 expression vector resulted in a dose-dependent transactivation of *MSX1* and *TGF-β3* reporter genes to a maximum of 8.5- and 7.3-fold above basal, respectively. A similar trend was observed when cells were co-transfected with vectors expressing FOXE1 with different polyalanine-stretch lengths, whereas S57N and R72S FOXE1 mutant plasmids exhibited a partial preservation of the transactivating function on both the promoters, achieving ~50% of the maximal transcriptional response obtained with the wt FOXE1. On the contrary, the F137S, the R102C and the A65V mutant FOXE1 showed negligible function. Therefore, the transactivation of *MSX1* and *TGF-β3* by FOXE1 is impaired by mutations in the DNA-binding motif.

Binding of FOXE1 to its responsive elements on *MSX1* and *TGF-β3* promoter regions

Promoter analysis of the main genes involved in palate development revealed one putative FOXE1 consensus site

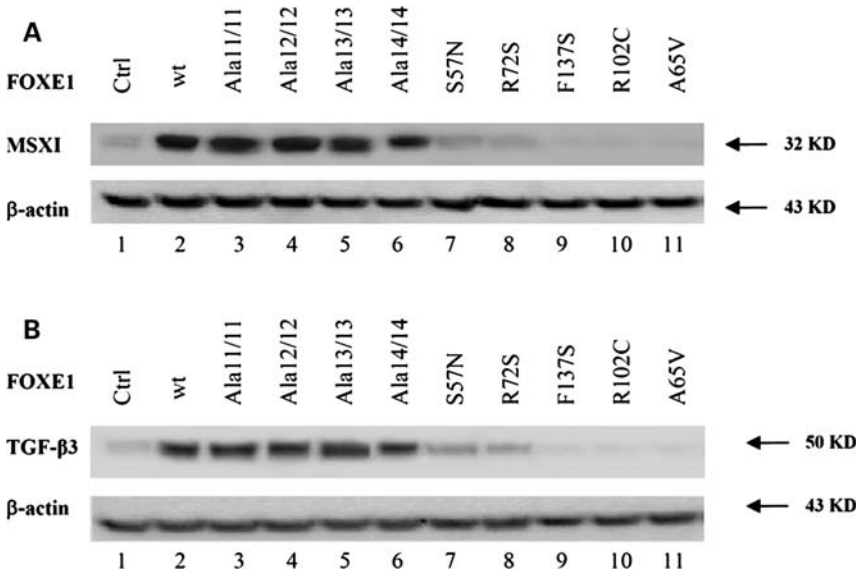

Figure 2. Western blot analysis of MSX1 and TGF-β3 proteins in 293 EBNA cells overexpressing wt or mutant FOXE1. Total lysate samples prepared from EBNA cells 36 h after transfection with pcDNA 3.1/V5 His wt or mutant FOXE1 expression vectors were equalized for protein loading according to expression before probing for MSX1 and TGF-β3. Proteins were resolved by 10% SDS–PAGE and immunoblotted using anti-MSX1 and anti-TGF-β3 rabbit polyclonal antibodies. Blots shown are representative of five independent experiments.

in the *MSX1* promoter from −612 to +608 and two FOXE1-binding motifs in the *TGF-β3* promoter from −1336 to −1332 and from −1217 to −1213 relative to the respective transcription start site (+1). All of them harbored the FOXE1 core sequence aaaca matching the FOXE1 consensus sequence within *Tg* and *TPO* promoters. On the basis of this information, we designed three wt double-stranded oligonucleotides containing the protected sequence which were used as substrates to detect specific DNA–protein complexes in band-shift assay (probe A within the *MSX1* promoter, and probes B and C within the *TGF-β3* promoter), two probes mutated in the core-binding motif (Mut A1 and B1) and two probes mutated in the flanking nucleotides (Mut A2 and B2), as reported in Table 1. The formation of a strong DNA–protein complex in extracts from EBNA cells transfected with the wt or the variable-polyalanine-stretch FOXE1 vectors was observed with probes A (Fig. 4A, lanes 2, 4, 6, 8 and 10) and B (Fig. 4B, lanes 2, 4, 6, 8 and 10), whereas no binding was detected with probe C (Fig. 4B, lane 21). A weaker but specific DNA–protein complex with probes A (Fig. 4A, lanes 12 and 14) and B (Fig. 4B, lanes 12 and 14) was found in cells overexpressing S57N and R72S mutant FOXE1. Negligible binding was detected in extracts from cells transfected with the F137S, the R102C and the A65V mutant FOXE1 (Fig. 4, sections A and B, lanes 16–18). The specificity of all the DNA–protein complexes was shown by supershift assays with the anti-V5 antibody (Fig. 4, sections A and B, lanes 3, 5, 7, 9, 11, 13 and 15). A severe DNA-binding deficit was observed when mutated probes (Mut A1, A2, B1 and B2) were employed (Fig. 4, sections A and B, lanes 19 and 20). The complex formation could be competed out by 100-fold excess unlabeled wt probes A (Fig. 4A, lane 21) and B (Fig. 4B, lane 22), and not by competing with mutant probes A1 (Fig. 4A, lane 22) and B1 (Fig. 4B, lane 23), thus strengthening the specificity of the results. Western blotting of the nuclear extracts used in the EMSA assays showed equivalent nuclear expression of wt and mutant FOXE1 proteins (Fig. 4C), suggesting that the observed differences in DNA binding were not due to variation in cellular expression of these proteins.

FOXE1 functionally interacts *in vivo* with *MSX1* and *TGF-β3* promoters

To study the potential role of FOXE1 as a direct transcriptional regulator of *MSX1* and *TGF-β3*, we performed ChIP experiments to detect the *in vivo* binding of the transcription factor to the *MSX1* and *TGF-β3* promoters. Figure 5 shows a marked interaction of FOXE1 with both the promoters in cells overexpressing the wt (lane 2, top and bottom panels) and the variable-polyalanine-stretch FOXE1 (lanes 3–6, top and bottom panels) and a significantly weaker binding in cells overexpressing the S57N and R72S mutant FOXE1 (lanes 7 and 8, top and bottom panels). Conversely, no binding was found in cells transfected with the F137S, the R102C and the A65V mutant FOXE1 vectors (lanes 9–11, top and bottom panels).

Foxe1 is involved in controlling Msx1 and Tgf-β3 expression in the horizontal palatal shelves in mouse embryos

In order to assess *in vivo* the role of *FOXE1* in controlling the expression of *MSX1* and *TGF-β3* genes, we studied the expression patterns of these two candidate target genes in the developing palatal shelves of *Foxe1*$^{-/-}$ mouse embryos. Whereas in 14-day *Foxe1*$^{+/-}$ embryos a strong Msx1 and Tgf-β3 expression was seen in maxillary molar dental

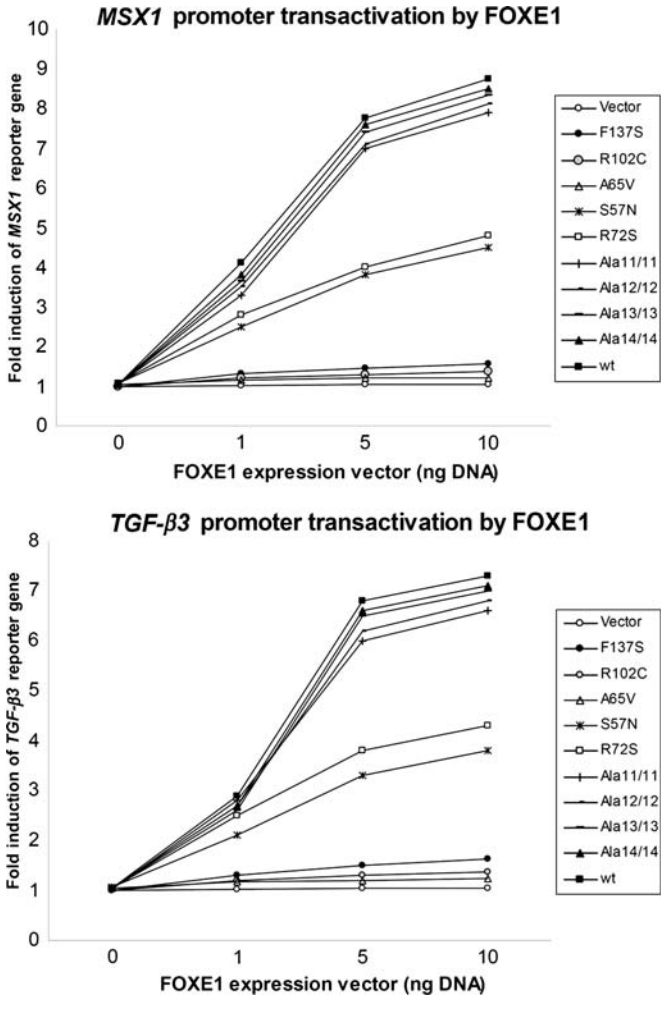

Figure 3. Transcriptional activity of wt or mutant FOXE1 on the human *MSX1* and *TGF-β3* promoters. 293 EBNA cells were co-transfected with 1 μg of *MSX1* or *TGF-β3* reporter genes together with increasing amount (1–10 ng) of empty pcDNA3, wt or mutant FOXE1 expression vectors. Luciferase activities were normalized for galactosidase values in three experiments each done in triplicate. Transcriptional activation by empty expression vector, and wt or mutant FOXE1 expression plasmids is shown as fold activity (mean ± SD) relative to cells transfected with reporter and no expression vector.

mesenchyme and in the epithelial cells of the anterior palate shelves, respectively (Fig. 6A and C), in *Foxe1* null embryos a great decrease of Msx1 and a lack of Tgf-β3 transcripts were detected (Fig. 6B and D).

DISCUSSION

In a search for potential downstream mediators of *FOXE1* function involved in the pathogenesis of craniofacial abnormalities seen in the Bamforth–Lazarus syndrome, we have identified *MSX1* and *TGF-β3* as novel *FOXE1* target genes. In developing vertebrate embryos, MSX1 and TGF-β3 are widely expressed at the sites where epithelial–mesenchymal interactions take place, including the cellular primordia involved in the craniofacial morphogenesis (22–24). Msx1 expression was observed in the first upper molar site in the mouse palatal mesenchyme (25), in the neural crest-derived

Table 1. Sequence alignment of wt (A, B and C) and mutated (Mut A1, A2, B1 and B2) oligonucleotides used as EMSA probes with the putative FOXE1-binding sites identified previously in thyroglobulin (Tg) and thyroperoxidase (TPO) promoters (19)

Oligo name	Sequence (5′ → 3′)
K sequence (Tg)	TGACTAGCAGAGAAAACAAAGTGA
Z sequence (TPO)	ACAAATACTAAACAAACAGAATGG
A[a]	AGTAGAGGAGAGAAACAAGGACG
Mut A1	AGTAGAGGAGAG**TCTT**AAGGACG
Mut A2	AGTAGAGG**TTCT**AAACAAGGACG
B[b]	CCTGTGCCTGTTTAAAACATTAACATCGTGCAG
Mut B1	CCTGTGCCTGTTTA**TCTT**ATTAACATCGTGCAG
Mut B2	CCTGTGCCTG**GGCT**AAACATTAACATCGTGCAG
C[b]	GTAACTTTCCAGAAAAACACCAACGTGTGGCAG

The putative FOXE1-responsive element is underlined. The mutated sequences are shown in bold.
[a]Corresponding to the putative FOXE1-binding site within the *MSX1* promoter.
[b]Corresponding to the two putative FOXE1-binding sites within the *TGFβ3* promoter.

mesenchyme surrounding the optic vesicle and in the surface epithelium adjacent to the vesicle (26). Antisense attenuation of Msx1 during early stages of neurulation produced hypoplasia of the maxillary, mandibular and frontonasal prominences, eye anomalies and somite and neural tube abnormalities (27). In addition, homozygous mice knockout for *Msx1* manifest a cleft secondary palate, a deficiency of alveolar mandible and maxilla, a failure of tooth development and also abnormalities of the nasal, frontal and parietal bones and of the malleus in the middle ear (28). In humans, mutations in the *MSX1* gene are associated with isolated non-syndromic cleft palate and tooth agenesis (29–32). Tgf-β3 is specifically expressed in murine medial edge epithelial cells of pre-fusion shelves, but its expression decreases shortly after the midline epithelial seam is formed (33–35). Depletion of Tgf-β3, through the use of either antisense oligonucleotide or neutralizing antibodies, prevents palatal fusion (36). In addition, the defects in epithelial–mesenchymal interactions associated with cleft palate have been shown in mice lacking in *Tgf-β3* (37,38). A single-nucleotide polymorphism, defined by the endonuclease SfaN1 and identified in intron 5 of *TGF-β3* (IVS5+104 A>G), was significantly associated with the increased risk of non-syndromic cleft lip/palate among the Korean population (39). An impairment of TGF-β3 expression was found in ectodermal derivates of non-syndromic cleft patients compared with controls, suggesting an alteration of *TGF-β3* action in this condition (40). Moreover, *TGF-β3* signaling is crucial for proper differentiation and morphogenesis of neural crest-derived cells in eye structures (41).

A previous study showed that in G401 kidney cell line, FOXE1 overproduction stimulates expression of 17 genes which do not include *MSX1 and TGF-β3*, but it did not specify whether in this cell line a basal expression of these genes occurs (42). In cells utilized in our experiments, basal levels of the two transcripts could be detected (Fig. 1) and we showed that they greatly increased after transfection with FOXE1-overexpressing plasmids. Moreover, the FOXE1-stimulated genes reported by Hishimuma *et al*. (42) are not involved in the palatal fusion, such as *WNT5A,* the other non-thyroid FOXE1-upregulated gene implicated in a

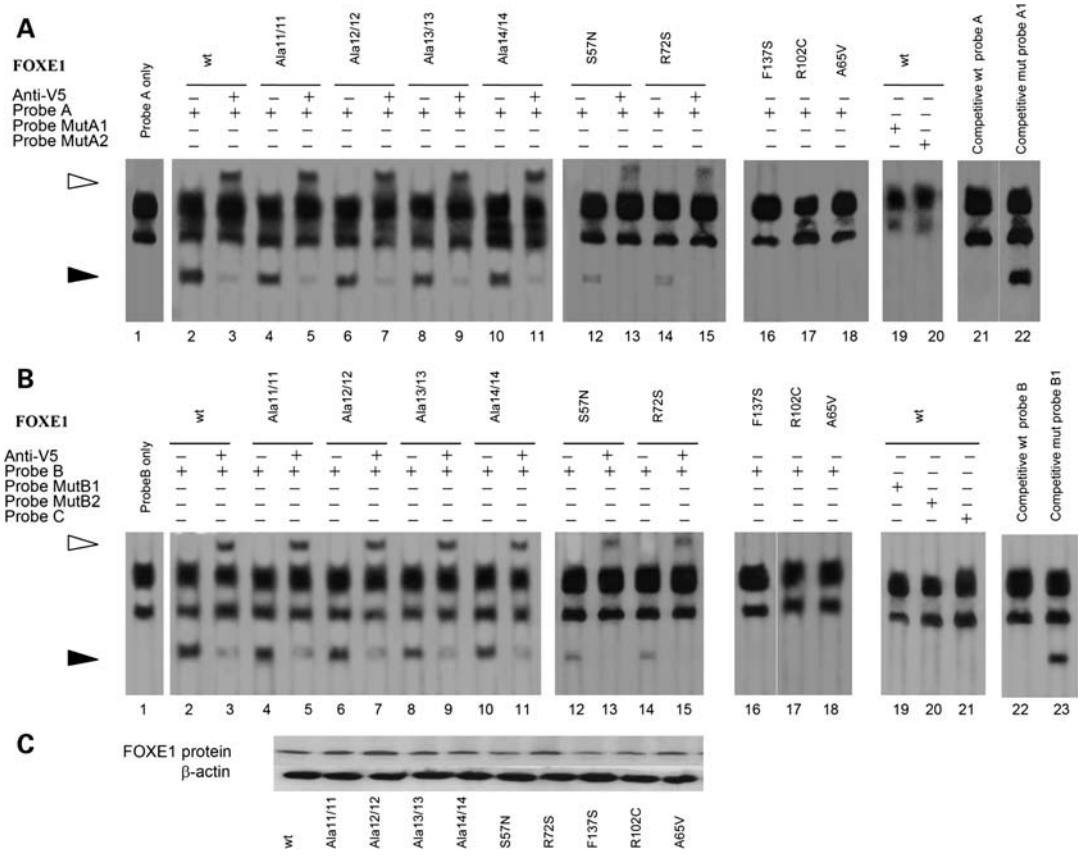

Figure 4. FOXE1 *in vitro* binding to *MSX1* and *TGF-β3* promoter regions. (**A** and **B**) Biotin-labeled oligonucleotide wt or mutant probes corresponding to the putative FOXE1-binding sites in the *MSX1* (section A) or *TGF-β3* (section B) promoters were incubated with nuclear extracts from 293 EBNA cells transfected with wt or mutant FOXE1 pcDNA3.1/V5-His-TOPO expression vectors. In supershift analysis, the anti-V5 antibody (2 μg) was incubated at room temperature (for 20 min) with the nuclear extracts prior to probe addition (lanes 3, 5, 7, 9, 11, 13 and 15). For competition assays, 100-fold excess of unlabeled wt or mut probes were incubated with nuclear extracts at room temperature 10 min before the addition of labeled probe (section A, lanes 21 and 22; section B, lanes 22 and 23). The solid arrowhead indicates a specific complex between wt or mutant FOXE1 and the oligonucleotide probe, whereas the blank arrow denotes this complex supershifted by the anti-V5 antibody. Wt and mutant probes are described in Table 1. (**C**) Western blot of the same nuclear extracts used in sections A and B, showing the wt or mutant V5-His-FOXE1 proteins.

Figure 5. *In vivo* binding of FOXE1 to the *MSX1* and *TGF-β3* promoters. The interaction of FOXE1 with *MSX1* and *TGF-β3* promoter sequences was evaluated using a ChIP assay. Aliquots of ChIPs immunoprecipitated with anti-V5 antibody from untransfected 293 EBNA cells (ctr) or cells transfected with wt or mutant FOXE1 expression vectors were amplified through PCR of the *MSX1* (top panel) or *TGF-β3* (bottom panel) promoters. Lane 12 contained IgG antibody for immunoprecipitation (negative control). Lane 13 is the 'input' lane where no immunoprecipitation was performed prior to PCR (positive control).

variety of human tumors (43). To our knowledge, this is the first evidence regarding the implication of genes involved in the palate fusion in executing the transcriptional program triggered by *FOXE1*.

The presence of FOXE1-binding sites in the promoter regions of *MSX1* and *TGF-β3* has been shown through the formation of specific DNA–protein complexes when nuclear extracts from FOXE1-transfected EBNA cells were incubated with probe A, reproducing the single putative binding sequence on *MSX1* promoter, and probe B, corresponding to one of the two putative consensus sites on *TGF-β3* promoter (Fig. 4). On the contrary, probe C, reproducing the other putative FOXE1-binding

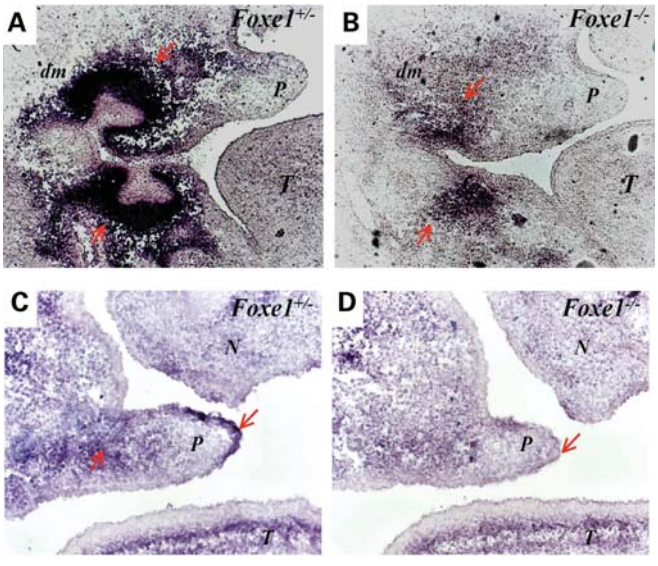

Figure 6. Msx1 and Tgf-β3 expression in the developing palatal shelves in the presence or absence of *Foxe1*. Coronal sections of E14 *Foxe1*$^{+/-}$ (**A** and **C**) and *Foxe1*$^{-/-}$ (**B** and **D**) embryos. (A) Msx1-intensive labeling was seen in the maxillary molar dental mesenchyme (arrows), but was not detected in the epithelia of palatal shelf. (B) The number of Msx1-positive cells (arrows) in the dental mesenchyme greatly decreased compared with normal mice (*Foxe1*$^{+/-}$). (C) Tgf-β3 transcript was detected in dispersed mesenchymal cells of developing palate shelf (arrow). Strong Tgf-β3 expression was seen in the epithelial cells of the anterior palate shelves (arrow). (D) The epithelial component of the palatal shelves (arrow) lacks the expression of Tgf-β3 in the absence of *Foxe1*. N, nasal septum; P, palatal shelves; dm, dental mesenchyme; T, tongue.

sequence on *TGF-β3* promoter, did not interact with wt FOXE1 protein even though it harbors the aaaca core motif present in the FOXE1 consensus site on *Tg* and *TPO* promoters (17,19). So, it appears that the flanking sequences are decisive for the specific DNA–protein complex formation. The specificity of the binding was further demonstrated by the lack of interaction when probes mutated either in the core motif or in the flanking nucleotides were employed. Thus, our observations led to the general belief that the protected sequences are necessary, but not sufficient enough, to ensure the transcription factor binding, since different positions flanking the core create differences in DNA-binding specificity (44). Moreover, we showed that FOXE1-binding ability was significantly decreased in cells overexpressing S57N or R72S mutants, whereas it was completely abolished when F137, R102C and A65V expression plasmids were transfected (Fig. 4).

The naturally occurring recruitment of FOXE1 to the *MSX1* and *TGF-β3* promoters was shown by specific PCR amplifications of both the promoter regions in EBNA cells overexpressing FOXE1. Interestingly, a robust amplification was observed in cells transfected with wt or variable-alanine-length FOXE1 plasmids, and a weak signal was detected in cells overexpressing the S57N or the R72S mutant FOXE1. No interaction occurred in cells transfected with the F137S, R102C and A65V expression plasmids (Fig. 5).

The binding we showed was functionally active as it was demonstrated by the ability of the wt and the variable-polyalanine-stretch FOXE1 expression vectors to increase *MSX1* and *TGF-β3* reporter gene transcription in a dose-dependent manner (Fig. 3). Conversely, a reduced or abolished luciferase expression occurred in cells co-transfected with the S57N and R72S, or F137S, R102C and A65V mutant FOXE1 expression vectors, respectively.

All these findings provide a strong indication that some craniofacial defects present in the Bamforth–Lazarus syndrome may be due to an altered transactivation function of the mutant FOXE1 on *MSX1* and *TGF-β3* transcription. This hypothesis is further supported by the strong induction of *MSX1* and *TGF-β3* at mRNA and protein levels in response to wt or variable-polyalanine-stretch FOXE1, and by a significantly impaired transcript and protein amounts of these two genes in cells transfected with the FOXE1 constructs differently mutated in the forkhead domain (Figs 1 and 2). These data point to a direct regulation of *MSX1* and *TGF-β3* by *FOXE1*.

The results reported here about the FOXE1 transcriptional activity on *MSX1* and *TGF-β3* genes reproduce the data obtained by others on *Tg* and *TPO* promoters (13–15,45). The S57N, F137S, R102C and A65V mutations within the forkhead DNA-binding domain of *FOXE1*, naturally occurring in the various Bamforth–Lazarus syndrome forms, differently impaired the transcription factor ability to bind to the promoters of the two thyroid-specific genes and to activate the transcription (12–15). The R72S-induced mutation in the DNA-binding region caused reduced expression of the *Tg* reporter, whereas the variable-polyalanine-stretch polymorphisms kept the FOXE1-binding and the transcriptional activities against this gene (45).

The *in situ* hybridization experiments performed by us in *Foxe1* knockout mice (Fig. 6) definitively elucidated the full significance of *FOXE1* gene integrity at the onset of the cleft palate in the Bamforth–Lazarus syndrome. The transcripts of genes certainly responsible for a correct palate development, such as *MSX1* and *TGF-β3*, are drastically reduced or absent in maxillary molar dental mesenchyme and in the epithelial cells of the anterior palate shelves in *Foxe1*$^{-/-}$ embryo mice 4 days before the complete fusion of the secondary palate with the primary palate anteriorly and with the nasal septum dorsally (46).

Therefore, taken together, our data allow to state that *MSX1* and *TGF-β3* are downstream targets of FOXE1. As these genes affect the organogenesis of several craniofacial structures, it may be conceivable that some attributes of the Bamforth–Lazarus syndrome, namely cleft palate, choanal atresia and ocular hypertelorism, otherwise not justified by *FOXE1* regulation of thyroid-specific genes, are dependent on the impairment of the mutant FOXE1 to transact *MSX1* and *TGF-β3* genes. Thus, evidence presented in this study leads us to believe that *MSX1* and *TGF-β3* genes are responsible for the onset of the craniofacial defects associated with this condition through the *FOXE1*-mediated regulation.

MATERIALS AND METHODS

Cells and culture conditions

293 EBNA cells (ECACC No. 85120602) were grown in Dulbecco's modified Eagle's medium (Sigma-Aldrich, Milan, Italy), supplemented with 10% fetal bovine serum

(Sigma-Aldrich), 50 IU/ml penicillin (EuroClone, Milan, Italy), 50 μg/ml streptomycin (EuroClone) in 5% CO_2 at 37°C. Cells were routinely tested for mycoplasma infection, and cultures were renewed, from frozen stocks, every 2 months.

Plasmid construction and transient transfection assays

Wild-type (wt) FOXE1 expression vectors were constructed by cloning into a pcDNA 3.1/V5 His expression vector (TOPO TA; Invitrogen, Carlsbad, CA, USA) the PCR products obtained from human genome using the forward primer 5′-ATGACTGCCGAGAGCGGGCCGCCGC-3′ and the reverse primer 5′-TCACATGGCGGACACGAACCGA TCTATC-3′. The mutants S57N, F137S, R102C and A65V FOXE1 were generated by site-directed mutagenesis of the wt *FOXE1* template using the QuikChange Site-Directed Mutagenesis Kit (Stratagene, Milan, Italy). Expression vectors of *FOXE1* tagged at the amino terminus with a V5 epitope tag were constructed by using the forward primer 5′-ATGACTGCCGAGAGAGCGGGCCGCCGC-3′ and the reverse primer 5′-CATGGCGGACACGAACCGATCTATCC CA-3′. *FOXE1* expression vectors with the R72S mutation in the forkhead domain or with variable-polyalanine-stretch lengths (11–14 residues) were kindly provided by Dr Hishinuma (Department of Clinical Laboratory Medicine, Tokyo, Japan).

MSX1 reporter vector was generated by PCR using forward primer 5′-ATTGAGCTCAGCTTCTCCCCGCAAGTTTA CTCC-3′ and reverse primer 5′-ATTAAGCTTCTCTCGGC TTTGACGAGCGGATC-3′. PCR conditions were 35 cycles at 94°C for 45 s, 52°C for 45 s, 72°C for 60 s and a final extension at 72°C for 10 min. The −542/+784 bp *MSX1* fragment with *Sac*I–*Hin*dIII termini was cloned into PGL2 basic vector (Promega, Milan, Italy). PGL3 plasmid containing the region −1454/−995 bp of *TGF-β3* promoter was kindly provided by Dr Labrie (Centre de Recherche en Endocrinologie Moléculaire et Oncologique, Québec, Canada). All constructs were verified by direct sequencing (CEQ 2000, Beckman Coulter, Milan, Italy).

293 EBNA cells were cultured in 35 mm well plates (5×10^5 cells/well) and transiently transfected with 1 μg reporter gene and 1–10 ng of wt or mutant FOXE1 expression vectors by using DMRIE (Invitrogen, Milan, Italy) according to the manufacturer's instructions. After 36–48 h, cells were harvested and protein extracts were prepared for the luciferase activity using luciferine (Promega) as the substrate. Luciferase activity was normalized for β-galactosidase activity produced by co-transfected pnls-LacZ plasmid.

RNA extraction and reverse transcription

293 EBNA cells were cultured in 35 mm well plates (2×10^6 cells/well) and transiently transfected with wt or mutated FOXE1 expression vectors. Total RNA was extracted with TRIzol (Invitrogen, Italy) according to the manufacturer's instructions. In a total volume of 20 μl, 1 μg of total RNA was reverse-transcribed with an IMProm-IITM reverse transcriptase kit (Promega) according to the manufacturer's instructions.

Quantitative real-time PCR

Quantitative real-time PCR was performed using the ABI Prism 7500 Real-Time PCR System (Applied Biosystems, Milan, Italy). We used 5′-CCTCTTTGCTCCCTGAGTTCA-3′ (forward primer), 5′-GGGACTCTTCCAGCCACTTTTT-3′ (reverse primer) and FAM-5′-CGAAGTCTGATCCCTG-3′-MGBNFQ as primers and a TaqMan probe for MSX1 (NCBI reference sequence: NM_002448), and 5′-GGAAGA AGCGGGCTTTGG-3′ (forward primer), 5′-GGGCGCACA CAGCAGTTC-3′ (reverse primer) and FAM-5′-AATTACT GCTTCCGCAACT-3′-MGBNFQ as primers and a TaqMan probe for TGF-β3 (NCBI reference sequence: NM_ 003239.2). Thermal cycling conditions included activation at 95°C (10 min) followed by 40 cycles each of denaturation at 95°C (15 s) and annealing/elongation at 60°C. Each sample was analyzed in triplicate with beta actin (Applied Biosystems) as an inner control, and the mean values of MSX1 and TGF-β3 mRNA were calculated. The cycle threshold (Ct) was used to calculate relative amounts of target DNA. The Ct was determined as the number of PCR cycles required for a given reaction to reach an arbitrary fluorescence value within the linear amplification range.

Chromatin immunoprecipitation assay

The chromatin immunoprecipitation (ChIP) enzymatic assay (Active Motif, Milan, Italy) was carried out, and the sheared chromatin samples obtained from EBNA cells overexpressing wt or mutant FOXE1 were used for immunoprecipitation with 2 μg of anti-V5 antibody (Invitrogen, Italy) overnight at 4°C. Immunocomplexes were subjected to cross-link reversal, extracted and precipitated as described in the protocol. The eluted DNA and the aliquots of chromatin prior to immunoprecipitation (input) were amplified by PCR. The forward primer 5′-TCCTAGGATAATAGCCATGC-3′ and the reverse primer 5′-TTCCTTCTCCTCTGCCCT-3′ were used to detect the DNA segment located at −788/−527 of *MSX1* promoter (NCBI reference sequence: NT_006051.17). The forward primer 5′-TCAGCTACCACGTCGAACGAGAG-3′ and the reverse primer 5′-TCCCTCCCATGACGTCTCTGGCCT-3′ were used to detect the DNA segment located at −1290/−1134 of *TGF-β3* promoter (NCBI reference sequence: M60556). The PCR conditions were as follows: 95°C for 4 min and 38 cycles of 94°C for 50 s, 65°C for 50 s and 72°C for 1 min. PCR products were separated by 2% agarose gel containing ethidium bromide.

Electrophoretic mobility shift assays

Nuclear extracts were prepared from 293 EBNA cells expressing wt or mutated V5-His epitope-tagged *FOXE1* (10 μg) using NE-PER Nuclear and Cytoplasmic Extraction Reagents (Pierce Biotechnology, Inc., Rockford, IL, USA) and stored at −80°C until use. Electrophoretic mobility shift assay (EMSA) was performed using the LightShift Chemiluminescent EMSA Kit (Pierce Biotechnology, Inc.) according to the provided instructions. The 5′-biotin-labeled oligonucleotide probes employed are reported in Table 1. Binding reaction mixture containing 3 μg of nuclear extract, 20 fmol of 5′-biotin-

labeled oligonucleotide probe(s), 1X binding buffer, 50 ng of poly(dI•dC), 2.5% glycerol, 0.05% NP-40 and 5 mM $MgCl_2$ was incubated at room temperature for 20 min in 20 μl of total reaction volume. For the antibody supershift assay, nuclear extracts were incubated with anti-V5 mouse monoclonal antibody (2 μg; Invitrogen, Italy) at room temperature (for 20 min) prior to probe addition. For competition assay, 100-fold excess unlabeled double-stranded oligonucleotides, used as competitors, were incubated with the extracts at room temperature 10 min before probe addition. Bound complexes were separated on 8% polyacrylamide gels, blotted onto nylon membrane and visualized on X-ray film (Fuji Hyperfilm, Naples, Italy).

Western blot analysis

Nuclear or total extract proteins were resolved by 10% SDS–PAGE and electroblotted onto Hybond ECL membrane (Amersham Biosciences, Milan, Italy). The blots were incubated with primary anti-V5 mouse monoclonal antibody (Invitrogen, Italy) or with rabbit polyclonal antibodies to MSX1 and TGF-β3 (AbCam, UK), according to the manufacturer's instructions. Mouse anti-β-actin monoclonal antibody (Sigma-Aldrich, Milan, Italy) was used to normalize protein loading to that of specific proteins in each lane. After overnight incubation at 4°C, membranes were washed with Tris-buffered saline/Tween and incubated with horseradish peroxidase-conjugated donkey anti-rabbit (Amersham Biosciences) or goat anti-mouse (Cell Signaling Technology, Milan, Italy) IgG as secondary antibodies at a dilution of 1:10 000 for 1 h at room temperature. The proteins were visualized with reagents from Pierce (Supersignal West Pico Chemiluminescent Substrate System, Pierce).

Animals

Foxe1 knockout mice have been previously described (10). Heterozygous male and female mice in C57BL/6 background were mated overnight, and the appearance of the vaginal plug was taken as day 0 of embryogenesis (E0). Pregnant mice were killed by cervical disclocation on E14. The heads of the fetuses were dissected, fixed overnight in 4% paraformaldehyde, equilibrated in 30% sucrose overnight at 4°C and embedded in OCT (Sakura), then specimens were quick-frozen over dry ice/ethanol slurry and stored at −80°C. Serial sections were taken in the frontal plane at 10 μm and processed for *in situ* hybridization.

Genotyping

Genotypes of *Foxe1* mutant embryos were determinated by PCR using genomic DNA isolated from yolk sacs as described (10).

Probe template PCR

DNA templates were generated from a cDNA derived by a reverse transcription of mRNA from E10.5 mouse embryos. In the PCR reaction, *MSX1* (forward: 5′-ATGGCCCCGGC TGCTGCTATG-3′; reverse: 5′-GCGGGGAGAAGCGGGG ACTCT-3′)- and *TGF-β3* (forward: 5′-GATGCACTTGCA AAGGGC-3′; reverse: 5′-CTCCATTGGGCTGAAAGG-3′)-specific forward and reverse primers extended at their 5′ end with either T7 or SP6 promoter sequences were used (T7, GAATTTAATACGACTCACTATAGGGAGA; SP6, CGAT TTAGGTGACACTATAGA). The best annealing temperature was determined by running an analytical (gradient) PCR in a range of 55–65°C. The resulting product was analyzed and purified on an agarose gel, and the desired band was extracted using the QIAGEN gel extraction kit (QIAGEN). Initial PCR products were re-amplified in a new PCR reaction. Templates were purified using QIAquick PCR Purification Kit (QIAGEN) and analyzed on an agarose gel. PCR products were sequence-verified.

RNA probe synthesis

In vitro transcription reaction for the synthesis of anti-sense RNA DIG-labeled probes was carried out according to the manufacturer's specifications (Roche). Briefly, 20 μl of master mix for each probe template was prepared to contain final concentrations of 1 mM ATP, CTP, GTP, 0.65 mM UTP, 0.35 mM DIG-11-UTP, 1X transcription buffer, 1 unit/μl RNase inhibitor, 20 unit/μl T7 or Sp6 RNA polymerase and 0.5 μg of above purified DNA templates, after which each of the samples was incubated at 37°C (2 h). Two microliters of 10 unit/Al RNase-free DNase I were added to each sample, which was then incubated at 37°C (15 min) to remove the DNA template. RNAs were purified by G-25 Sephadex MiniQuick Spin Columns (Roche) and were analyzed on a 1% RNA denaturing gel for quality check, and their concentration was determined in a photometer. Labeling incorporation was checked by comparing the provided DIG-labeled control, following essentially the instructions of the labeling kit.

In situ hybridization

The sections were fixed in 4% PFA, washed in PBS-DEPC and treated with 1 μg/ml of Proteinase K (Roche) in PBS-DEPC for 10 min at room temperature. The sections were then subjected to acetylation step using 0.25% acetic anhydride (Sigma) in 1 M triethanolamine (Sigma)–HCL (J.T. Baker) for 10 min. Thereafter, slides were hybridized overnight at 68°C in the hybridization mix (50% formamide (EuroClone); 5X SSC, pH 4.5 (AppliChem); 50 μg/ml yeast tRNA (Roche); 1% SDS; 50 μg/ml heparin (Sigma), using a probe concentration of 0.5–1 μg/ml. Sections were incubated with anti-digoxigenin alkaline phosphatase-conjugated Fab fragments (Roche) at 1:4000 dilution. Staining was developed for 24/48 h, according to probe signal, with BM Purple AP Substrate (Roche). Finally, slides were fixed in 4% PFA–0.2% gluteraldehyde (Sigma) and mounted in glycerol (Dako). The *in situ* reaction was controlled under an AXIOPLAN 2 microscope equipped with Axiocam digital camera (Zeiss), and the images were processed using Axion Vision software and edited using ImageJ software.

Densitometry and statistical analysis

The relative intensities of protein and nucleic acid bands were analyzed using the Digital Sciences one-dimensional program from Kodak Scientific Imaging Systems (New Haven, CT, USA). Standard curves were run, and the data that were obtained were in the linear range of the curve. In addition, all of the values were normalized to their respective lane-loading controls. The data are expressed as the means ± SE of *n* determinations. The results were analyzed by two-tailed Student's *t* test. *P*-values <0.05 were considered significant.

ACKNOWLEDGEMENTS

We thank Dr Elisa Gerace (Department of Experimental Pathology and Microbiology, Section of Experimental Microbiology, University of Messina, Italy) for her technical support in preparing the luciferase reporter MSX1 gene and Dr Germana Cubeta for her linguistic assistance.

Conflict of Interest statement. None declared.

FUNDING

This work was supported by grants for the PhD research of D.T. on the 'Pathology of Cellular Proliferation and Differentiation' and by the School of Specialization in Clinical Pathology, University of Messina.

REFERENCES

1. Carlsson, P. and Mahlapuu, M. (2002) Forkhead transcription factors: key players in development and metabolism. *Dev. Biol.*, **250**, 1–23.
2. Carroll, J.S., Liu, X.S., Brodsky, A.S., Li, W., Meyer, C.A., Szary, A.J., Eeckhoute, J., Shao, W., Hestermann, E.V., Geistlinger, T.R. *et al.* (2005) Chromosome-wide mapping of estrogen receptor binding reveals long-range regulation requiring the forkhead protein FoxA1. *Cell*, **122**, 33–43.
3. Katoh, M. (2004) Human FOX gene family. *Int. J. Oncol.*, **25**, 1495–1500.
4. Lee, C.S., Friedman, J.R., Fulmer, J.T. and Kaestner, K.H. (2005) The initiation of liver development is dependent on Foxa transcription factors. *Nature*, **435**, 944–947.
5. Lehmann, O.J., Sowden, J.C., Carlsson, P., Jordan, T. and Bhattacharya, S.S. (2003) Fox's in development and disease. *Trends Genet.*, **19**, 339–344.
6. Chadwick, B.P., Obermayr, F. and Frischauf, A.M. (1997) FKHL15, a new human member of the forkhead gene family located on chromosome 9q22. *Genomics*, **41**, 390–396.
7. Zannini, M., Avantaggiato, V., Biffali, E., Arnone, M.I., Sato, K., Pischetola, M., Taylor, B.A., Phillips, S.J., Simeone, A. and Di Lauro, R. (1997) TTF-2, a new forkhead protein, shows a temporal expression in the developing thyroid which is consistent with a role in controlling the onset of the differentiation. *EMBO J.*, **16**, 3185–3197.
8. Dathan, N., Parlato, R., Rosica, A., De Felice, M. and Di Lauro, R. (2002) Distribution of the *titf2/foxe1* gene product is consistent with an important role in development of foregut endoderm, palate, and hair. *Dev. Dyn.*, **224**, 450–456.
9. Trueba, S.S., Augé, J., Mattei, G., Etchevers, H., Martinovic, J., Czernichow, P., Vekemans, M., Polak, M. and Attié-Bitak, T. (2005) *PAX8*, *TITF1*, and *FOXE1* gene expression patterns during human development: new insights into human thyroid development and thyroid dysgenesis-associated malformations. *J. Clin. Endocrinol. Metab.*, **90**, 455–462.
10. De Felice, M., Ovitt, C., Biffali, E., Rodriguez-Mallon, A., Arra, C., Anastassiadis, K., Macchia, P.E., Mattei, M.G., Mariano, A., Schöler, H. *et al.* (1998) A mouse model for hereditary thyroid dysgenesis and cleft palate. *Nat. Genet.*, **19**, 395–398.
11. Bamforth, J.S., Hughes, I.A., Lazarus, J.H., Weaver, C.M. and Harper, P.S. (1989) Congenital hypothyroidism, spiky hair, and cleft palate. *J. Med. Genet.*, **26**, 49–51.
12. Castanet, M., Mallya, U., Agostini, M., Schoenmakers, E., Mitchell, C., Demuth, S., Raymond, F.L., Schwabe, J., Gurnell, M. and Chatterjee, V.K. (2010) Maternal isodisomy for chromosome 9 causing homozygosity for a novel FOXE1 mutation in syndromic congenital hypothyroidism. *J. Clin. Endocrinol. Metab.*, **95**, 4031–4036.
13. Baris, I., Arisoy, A.E., Smith, A., Agostini, M., Mitchell, C.S., Park, S.M., Halefoğlu, A.M., Zengin, E., Chatterjee, V.K. and Battaloglu, E. (2006) A novel missense mutation in human TTF-2 (FKHL15) gene associated with congenital hypothyroidism but not athyreosis. *J. Clin. Endocrinol. Metab.*, **91**, 4183–4187.
14. Castanet, M., Park, S.M., Smith, A., Bost, M., Leger, J., Lyonnet, S., Pelet, A., Czernichow, P., Chatterjee, K. and Polak, M. (2002) A novel loss-of-function mutation in TTF-2 is associated with congenital hypothyroidism, thyroid agenesis and cleft palate. *Hum. Mol. Genet.*, **11**, 2051–2059.
15. Clifton-Bligh, R.J., Wentworth, J.M., Heinz, P., Crisp, M.S., John, R., Lazarus, J.H., Ludgate, M. and Chatterjee, V.K. (1998) Mutation of the gene encoding human TTF-2 associated with thyroid agenesis, cleft palate and choanal atresia. *Nat. Genet.*, **19**, 399–401.
16. Aza-Blanc, P., Di Lauro, R. and Santisteban, P. (1993) Identification of a cis-regulatory element and a thyroid-specific nuclear factor mediating the hormonal regulation of rat thyroid peroxidase promoter activity. *Mol. Endocrinol.*, **7**, 1297–1306.
17. Civitareale, D., Lonigro, R., Sinclair, A.J. and Di Lauro, R. (1989) A thyroid-specific nuclear protein essential for tissue-specific expression of the thyroglobulin promoter. *EMBO J.*, **8**, 2537–2542.
18. De Felice, M. and Di Lauro, R. (2004) Thyroid development and its disorders: genetics and molecular mechanisms. *Endocr. Rev.*, **25**, 722–746.
19. Francis-Lang, H., Price, M., Polycarpou-Schwarz, M. and Di Lauro, R. (1992) Cell-type-specific expression of the rat thyroperoxidase promoter indicates common mechanisms for thyroid-specific gene expression. *Mol. Cell. Biol.*, **12**, 576–588.
20. Santisteban, P., Acebron, A., Polycarpou-Schwarz, M. and Di Lauro, R. (1992) Insulin and insulin-like growth factor I regulate a thyroid-specific nuclear protein that binds to the thyroglobulin promoter. *Mol. Endocrinol.*, **6**, 1310–1317.
21. Sinclair, A.J., Lonigro, R., Civitareale, D., Ghibelli, L. and Di Lauro, R. (1990) The tissue-specific expression of the thyroglobulin gene requires interaction between thyroid specific and ubiquitous factors. *Eur. J. Biochem.*, **193**, 311–318.
22. Adab, K., Sayne, J.R., Carlson, D.S. and Opperman, L.A. (2002) Tgf-beta1, Tgf-beta2, Tgf-beta3 and Msx2 expression is elevated during frontonasal suture morphogenesis and during active postnatal facial growth. *Orthod. Craniofac. Res.*, **5**, 227–237.
23. Alappat, S., Zhang, Z.Y. and Chen, Y.P. (2003) *Msx* homeobox gene family and craniofacial development. *Cell Res.*, **13**, 429–442.
24. Berdal, A., Molla, M., Hotton, D., Aïoub, M., Lézot, F., Néfussi, J.R. and Goubin, G. (2009) Differential impact of MSX1 and MSX2 homeogenes on mouse maxillofacial skeleton. *Cells Tissues Organs*, **189**, 126–132.
25. Zhang, Z., Song, Y., Zhao, X., Zhang, X., Fermin, C. and Chen, Y. (2002) Rescue of cleft palate in *MSX1*-deficient mice by transgenic *BMP4* reveals a network of BMP and Shh signalling in the regulation of mammalian palatogenesis. *Development*, **129**, 4135–4146.
26. Monaghan, A.P., Davidson, D.R., Sime, C., Graham, E., Baldock, R., Bhattacharya, S.S. and Hill, R.E. (1991) The *Msh*-like homeobox genes define domains in the developing vertebrate eye. *Development*, **112**, 1053–1061.
27. Foerst-Potts, L. and Sadler, T.W. (1997) Disruption of Msx-1 and Msx-2 reveals roles for these genes in craniofacial, eye, and axial development. *Dev. Dyn.*, **209**, 70–84.
28. Satokata, I. and Maas, R. (1994) MSX1 deficient mice exhibit cleft palate and abnormalities of craniofacial and tooth development. *Nat. Genet.*, **6**, 348–356.
29. Blanco, R., Jara, L., Villaseca, C., Palomino, H. and Careno, H. (1998) Genetic variation of MSX1 has a sexual dimorphism in non-syndromic cleft palate in the Chilean population. *Rev. Med. Chil.*, **126**, 781–787.

30. Lidral, A.C., Romitti, P.A., Basart, A.M., Doetschman, T., Leysens, N.J., Daack-Hirsch, S., Semin, E.V., Johnson, L.R., Machida, J., Burds, A. *et al.* (1998) Association of MSX1 and TGF-β3 with nonsyndromic clefting in humans. *Am. J. Hum. Genet.*, **63**, 557–568.
31. Van den Boogaard, M.J., Dorland, M., Beemer, F.A. and van Amstel, H.K. (2000) MSX1 mutation is associated with orofacial clefting and tooth agenesis in humans. *Nat. Genet.*, **24**, 342–343.
32. Vastardis, H., Karimbux, N., Guthua, S.W., Seidman, J.G. and Seidman, C.E. (1996) A human MSX1 homeodomain missense mutation causes selective tooth agenesis. *Nat. Genet.*, **13**, 417–421.
33. Fitzpatrick, D.R., Denhez, F., Kondaiah, P. and Akhurst, R. (1990) Differential expression of TGF-β isoforms in murine palatogenesis. *Development*, **109**, 585–595.
34. Gehris, A., D'Angelo, M. and Greene, R.M. (1991) Immunodetection of the transforming growth factors β1 and β2 in the developing murine palate. *Int. J. Dev. Biol.*, **35**, 17–24.
35. Pelton, R.W., Hogan, B.L., Miller, D.A. and Moses, H.L. (1990) Differential expression of the genes encoding TGFs β1, β2, and β3 during murine palate formation. *Dev. Biol.*, **141**, 456–460.
36. Brunet, C.L., Sharpe, P.M. and Ferguson, M.W.J. (1995) Inhibition of TGF-β3 (but not TGF-β1 or TGF-β2) activity prevents normal mouse embryonic palate fusion. *Int. J. Dev. Biol.*, **39**, 345–355.
37. Kaartinen, V., Voncken, J.W., Shuler, C., Warburton, D., Bu, D., Heisterkamp, N. and Groffen, J. (1995) Abnormal lung development and cleft palate in mice lacking TGF-β3 indicates defects of epithelial–mesenchymal interaction. *Nat. Genet.*, **11**, 415–421.
38. Proetzel, G., Pawlowski, S.A., Wiles, M.V., Yin, M., Bolvin, G.P., Howles, P.N., Ding, J., Ferguson, M.W. and Doetschman, T. (1995) Transforming growth factor-β3 is required for secondary palate fusion. *Nat. Genet.*, **11**, 409–414.
39. Kim, M.H., Kim, H.J., Choi, J.Y. and Nahm, D.S. (2003) Transforming growth factor-beta3 gene SfaN1 polymorphism in Korean nonsyndromic cleft lip and palate patients. *J. Biochem. Mol. Biol.*, **36**, 533–537.
40. Rullo, R., Gombos, F., Ferraraccio, F., Farina, A., Morano, D., Festa, V.M., Guida, L., Martinelli, M., Scapoli, L., Pezzetti, F. and Carinci, F. (2006) TGFβ3 expression in non-syndromic orofacial clefts. *Int. J. Pediatr. Otorhinolaryngol.*, **70**, 1759–1764.
41. Ittner, L.M., Wurdak, H., Schwerdtfeger, K., Kunz, T., Ille, F., Leveen, P., Hjalt, T.A., Suter, U., Karlsson, S., Hafezi, F., Born, W. and Sommer, L. (2005) Compound developmental eye disorders following inactivation of TGFβ signalling in neural-crest stem cells. *J. Biol.*, **4**, 11.
42. Hishinuma, A., Ohmika, N., Namatame, T. and Ieiri, T. (2004) TTF-2 stimulates expression of 17 genes, including one novel thyroid-specific gene which might be involved in thyroid development. *Mol. Cell. Endocrinol.*, **221**, 33–46.
43. Katoh, M. and Katoh, M. (2009) Transcriptional mechanisms of WNT5A based on NF-kappaB, Hedgehog, TGFbeta, and Notch signaling cascades. *Int. J. Mol. Med.*, **23**, 763–769.
44. Ortiz, L., Zannini, M., Di Lauro, R. and Santisteban, P. (1997) Transcriptional control of the forkhead thyroid transcription factor TTF-2 by thyrotropin, insulin, and insulin-like growth factor I. *J. Biol. Chem.*, **272**, 23334–23339.
45. Hishinuma, A., Ohyama, Y., Kuribayashi, T., Nagakubo, N., Namatame, T., Shibayama, K., Arisaka, O., Matsuura, N. and Ieri, T. (2001) Polymorphism of the polyalanine tract of thyroid transcription factor-2 gene in patients with thyroid dysgenesis. *Eur. J. Endocrinol.*, **145**, 385–389.
46. Gritli-Linde, A. (2007) Molecular control of secondary palate development. *Dev. Biol.*, **301**, 309–326.